

Loss Performance of Intra-Vehicle Channels for Narrowband Signal Transmission

Irfan Yusoff, Xiao-Hong Peng and Jack Hydns

School of Engineering & Applied Science,
Aston University,
Birmingham, UK.
Email: mohdymni@aston.ac.uk, x-h.peng@aston.ac.uk

Abstract—In this paper, we examine the intra-vehicle radio propagation performance of narrowband signals at 2.4 GHz and 5.9 GHz. The measurements are taken from a vehicle testbed and analyzed based on the path loss model that comprises the mean, large-scale fading and small-scale fading loss components. We show that multipath fading, especially the small-scale fading, has the dominant impact on the loss performance, while the mean loss varies relative to the free-space loss in this environment. Different accumulated distribution functions are applied to assess their suitability for characterizing the large-scale and small-scale fading effects, and compared through the non-parametric tests.

Index Terms—Intra-vehicle channel characteristics, path loss model, large-scale fading, small-scale fading, testbed.

I. INTRODUCTION

Wireless communications have been introduced to vehicles, e.g.: Bluetooth and Wi-Fi are commonly used inside vehicles for infotainment, and the Global Navigation Satellite System (GNSS) is adopted for navigation. In addition, IEEE 802.11p and LTE-V2X systems [1] have been deployed to enable communication between vehicles (vehicle-to-vehicle or V2V) and between vehicles and roadside units (vehicle-to-infrastructure or V2I) for improving driving safety and data services to road users.

Applying wireless communication technologies inside a vehicle can improve its fuel and space efficiency through reducing wire harness which leads to the weight reduction and space saving for the vehicle. To achieve this end, the properties of intra-vehicle wireless channels need to be thoroughly investigated in order to develop appropriate technologies and protocols which can ensure the transmission performance required.

The aim of this work is to gain a better understanding of the characteristics of intra-vehicle channels for narrowband wireless signals in term of their distance-dependent attenuation factor and fading property at two different frequencies: 2.4 GHz and 5.9 GHz, which are chosen as they cover the 2.4 GHz unlicensed band and the 5.9 GHz dedicated short-range communications (or IEEE802.11p) band.

In addition, the investigation of the loss performance of the intra-vehicle channel is the focus of the empirical work we carried out. This will demonstrate that the overall path loss performance is contributed jointly by a mean loss component which follows the log-distance loss model, and multipath

fading, namely large-scale and small-scale fading, related loss components. We will also show the level of influence from each of these components over the overall loss performance at different frequencies.

We have chosen to study the narrowband performance as it has been largely overlooked as compared to the published work on the Ultra-Wideband (UWB) transmission [2]. It is important to understand the narrowband behavior of the intra-vehicle channel as the wireless systems used or recommended for vehicles such as Bluetooth (no more than 2 MHz for each channel), Zigbee (2 MHz for each channel) and Wi-Fi (20 or 22 MHz for each channel) are all in this range. Furthermore, our results on the narrowband characteristics will provide a better understanding of the flat or deep fading behavior in the intra-vehicle environment.

Although there have been some investigations on the propagation characteristic of narrowband signals in intra-vehicle wireless channels, most of them are more focused at the general behavior of this type of channels, such as channel coherent bandwidth, frequency diversity and power delay profile. Some exemplar investigations include the work carried out by Cheng et al. which produces a simple analytical multi-ray model with field measurements [3], and the work by Liu et al. which analyses the potential benefit of frequency diversity for intra-vehicle wireless applications [4].

In addition, a study by Moghimim et. al. [5] examines channel coherence time and channel loss statistics at 915 MHz and 2.4 GHz but without considering the distance related loss performance. Kamoda et al. have presented both UWB and narrowband channel models for the engine compartment only which can be very different from the passenger compartment in propagation characteristics as they commented [6].

Our work provides more insight into the causes of intra-vehicle channel behavior by revealing the location/distance based loss performance and the fading phenomenon in both small scale and large-scale aspects and, at the same time, showing how they collectively contribute to the loss performance in such a complicated environment.

The structure of the paper is organized as follows. Section II describes the testbed used for this research and related settings based on which the measurements were collected. The results, including path loss and channel fading characteristics,

TABLE I
USRP SETTINGS AT 2.4 GHz AND 5.9 GHz

Frequency Setting	2.45 GHz	5.9 GHz
Antenna	ANT-2.4-LCW-SMA	TG.35.8113
Tx Power	-0.8 dBm	-5.18 dBm
Tx Gain Setting	73	73
Rx Gain Setting	35	60
Sample Rate	10Msps	10Msps
Update Rate	1Msps	1Msps

are presented in Section III together with proper discussions. Finally, the paper is concluded in Section IV.

II. TESTBED AND EXPERIMENT

A. Testbed Setup

The testbed was set up within the passenger and boot compartments in a Land Rover Discovery vehicle and two Universal Software Radio Peripheral (USR) B210 devices from National Instruments were used as a transmitter and a receiver in the tests. Each USRP was connected to an omnidirectional antenna from Linx Technologies (2.4 GHz) and Taoglas Limited (5.9 GHz), and also attached to a laptop for signal generation and processing. The antennas were kept vertically polarised throughout the tests carried out with the transmitter and receiver aligned towards the back and front of the vehicle, respectively.

The transmitter was configured to transmit a baseband signal modulated by a carrier wave at the chosen frequency of 2.4 GHz or 5.9 GHz. The output power of the transmitter (USR) was calibrated in reference to the component datasheet of the USRP and through a laboratory measurement with a Tektronix spectrum analyzer. The output power is set to be -1 dBm at 2.4 GHz and -5 dBm at 5.9 GHz. The receiver was configured to receive the complex signal waveforms for a length of 10 seconds, which resulted in a total of 100 million received samples in the time domain for each testing location. The measurements were collected through three runs for each test. The related settings are summarized and specified in Table I.

B. Measurement Procedure and Scenario

A frequency spectrum scan was performed before taking measurements to ensure the chosen channel to be free from interference. The vehicle was in a stationary position with the engine and electric power turned off during the tests. The area around the vehicle was also kept out of any large objects and human movement throughout the tests.

The transmitter was placed at a fixed location on the dashboard of the vehicle, while the location of the receiver (USR) was changeable depending on the requirement in different tests. Two types of tests were conducted:

a) Test-1: Measuring the received signal power at 44 different locations across the passenger and boot compartments, as shown in Fig. 1, at 2.4 GHz and 5.9 GHz.

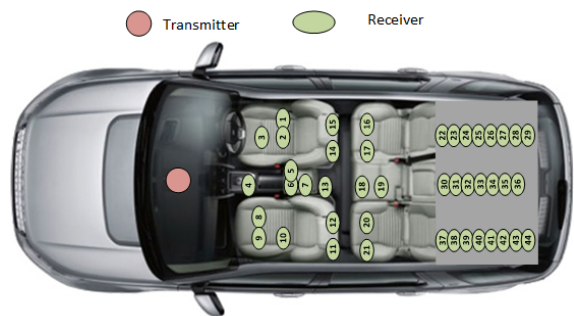


Fig. 1. Locations of 44 measurement points in Test-1.

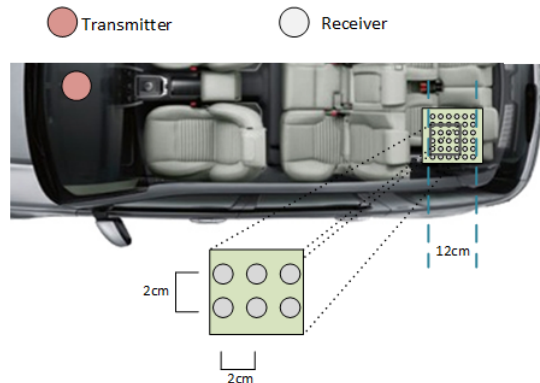


Fig. 2. Measurement grid of 12cm by 12cm (36 locations) for Test-2.

b) Test-2: Measuring the received signal power at 2.4 GHz in the boot compartment within a small 12cm x 12cm grid (36 locations with a separation distance of 2 cm between the marked locations), as shown in Fig. 2, for validating the loss component due to small-scale fading.

For each of the measurements taken, all necessary information such as the height and relative distance of the location was recorded and used later to calculate the separation distance between the transmitter and receiver antennas. The recorded results in the form of complex numbers were processed in MATLAB to extract the received power in dBm.

III. TEST RESULT AND ANALYSIS

A. Mean Path Loss

Path loss is frequently used to measure the propagation loss of radio signal transmission between a transmitter and a receiver. The intra-vehicle path loss behavior can be modelled by combining the mean path loss L_m , the loss due to slow or large-scale fading X_α , and loss due to fast or small-scale fading β_s . The combined path loss, denoted by L_p , is expressed by (all in dB):

$$L_p = L_m + X_\alpha + \beta_s \quad (1)$$

The mean path loss is defined by the generalized Friis equation also known as the log-distance path loss model, which comprises two parts: 1) the loss at a reference distance, d_0 ,

from the transmitter and 2) the loss logarithmically increasing with distance, which is given by [7]:

$$L_m = L_{ref}(d_0) + 10n \log_{10}\left(\frac{d}{d_0}\right) \quad (2)$$

where the terms L_{ref} , n , d , d_0 represents the path loss at a reference distance, the path loss exponent, the distance between the transmitter and receiver antennas, and the chosen reference distance, respectively.

By using the measurements collected from the 44 locations in Test-1, the mean path loss L_m can be estimated by using the Least Square Linear Regression method [8]. Base on Eq.(2), the mean loss value for each of the 44 locations (receivers), $L_{m,i}$, is obtained by:

$$L_{m,i} = L_{ref,i} + 10n_i x_i \quad \text{for } i = 1, 2, \dots, 44. \quad (3)$$

where

$$x_i = \log_{10}\left(\frac{d_i}{d_0}\right), \quad (4)$$

$$n_i = \frac{\sum_{i=1}^{44} (x_i - \bar{x})(L_i - \bar{L})}{\sum_{i=1}^{44} (x_i - \bar{x})^2}, \quad \text{and} \quad (5)$$

$$L_{ref,i} = \bar{L} - n_i \bar{x} \quad (\bar{L} = \frac{\sum_{i=1}^{44} L_i}{44}). \quad (6)$$

where d_i , L_i , represent the distance of i th location in meters and the instance path loss of the i th location in dB, respectively.

The path loss and estimated mean path loss which represent the first path loss component, L_m , are produced in Fig.3 for 2.4 GHz and Fig. 4 for 5.9 GHz. The reference distance is set to be $d_0 = 1$ meter. The extracted parameters for both 2.4 GHz and 5.9 GHz are shared and shown in Table II together with the loss at the reference distance, L_{ref} .

For comparison purposes, the results of the Friis model or the free-space loss model (L_f and $n = 2$) are also produced in Fig. 3 and Fig. 4, according to:

$$L_f = 20 \log_{10}\left(\frac{d}{d_0}\right) + 20 \log_{10}(f) + 20 \log_{10}\left(\frac{4\pi}{c}\right) \quad (7)$$

where f and c represent signal frequency and the speed of light, respectively. These results show that the mean path loss of the intra-vehicle narrowband transmission exhibits varied relationships with the free-space loss. At 2.4 GHz the mean loss is lower than the free-space loss by 2-4 dB over the 3 meters range in the vehicle, as shown in Fig. 3. However, when the frequency is increased to 5.9 GHz, the mean loss has a significantly larger increase than that of the free-space loss over the majority of the test range, as shown in 4. It is also observed that the special path loss performance inside vehicles, in terms of the scale of variation, is mainly contributed by the multipath fading effect which will be examined in detail in the following subsections.

TABLE II
ESTIMATED LOSS EXPONENT AND REFERENCE PATH LOSS

Frequency (GHz)	n	L_{ref} (dB)
2.4	2.212	37.04
5.9	1.289	50.43

TABLE III
GOODNESS OF FIT FOR LARGE-SCALE FADING (X_α)

Frequency: 2.4 GHz			
Distribution	KS	Chi	MLE
Log-normal	75.55%	23.25%	37.97%
Rayleigh	0.02%	5.44%	<0.01%
Rician	6.92%	23.85%	23.62%
Weibull	0.41%	23.67%	2.92%
Nakagami	17.10%	23.79%	35.5%
Frequency: 5.9 GHz			
Distribution	KS	Chi	MLE
Log-normal	91.17%	20.76%	65.06%
Rayleigh	0.1%	24.73%	<0.01%
Rician	1.92%	18.12%	7.92%
Weibull	<0.1%	16.98%	2.8%
Nakagami	6.72%	19.42%	24.22%

B. Large-scale fading

The large-scale fading also known as shadowing represents the local average slow fading characteristic of the received signal. It is defined in this analysis as the local-mean received signal power within a window of 50 cm which is equivalent to 4λ at 2.4 GHz and 10λ at 5.9 GHz, where λ denotes the wavelength. This window size is chosen base on the consideration that it should cover a enough number of measurements from neighboring locations in the test. But at the same time it should not be too wide as this will compromise the location differentiation factor, i.e. no obvious variation in loss can be identified between neighboring local mean values. The loss component due to large-scale fading is extrapolated using the Moving Mean method, with the metric given by [9]:

$$L_\gamma = \frac{1}{k} \sum_{i=1}^k L_i \quad (8)$$

where L_γ represents the local mean, k is the window size defined by the number of samples within the window, and L_i is the path loss of the i th sample. The large-scale fading results are shown in Fig. 3 for 2.4 GHz and Fig. 4 for 5.9 GHz, by the dashed lines.

In wireless communications, large-scale fading is normally described as a log-normal distributed random variable. But it has been argued that this is not always the case as other distribution functions have demonstrated a better fit in some scenarios. Therefore, we evaluated this performance using the Cumulative Density Function (CDF) of the Relative Loss Variation (RLV) against the mean path loss, and through the comparisons between different distribution functions such as

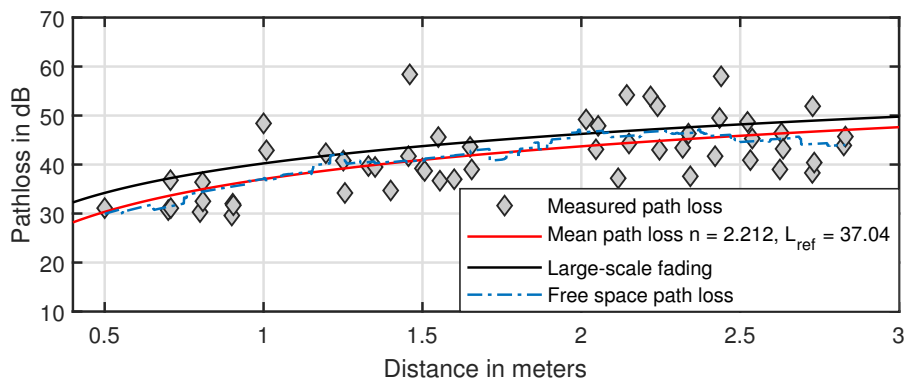


Fig. 3. Measured path loss, estimated mean path loss and loss due to large-scale fading at 2.4 GHz.

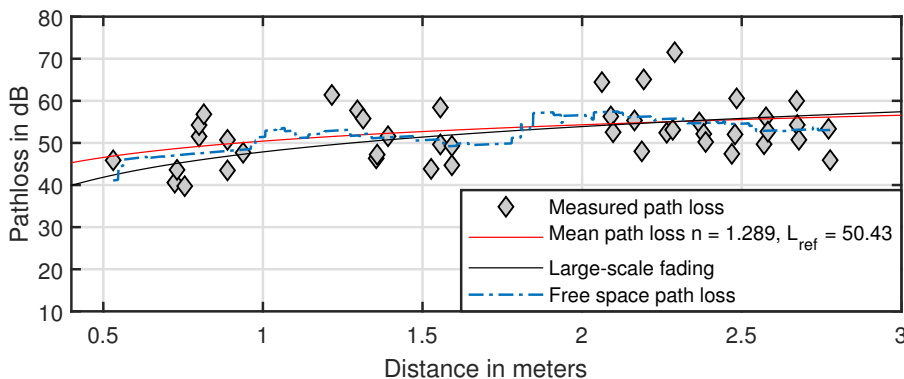


Fig. 4. Measured path loss, estimated mean path loss and loss due to large-scale fading at 5.9 GHz.

TABLE IV
PARAMETERS OF LOG-NORMAL DISTRIBUTION (NORMAL IN dB) FOR
LARGE-SCALE FADING (X_α) AT 2.4 GHz AND 5.9 GHz

Frequency(GHz)	Mean(dB)	Standard Deviation(dB)	Variance(dB)
2.4	0.0824	1.479	2.188
5.9	0.236	2.121	4.5

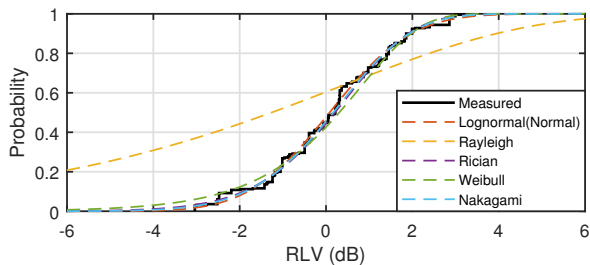


Fig. 5. CDF of relative loss variation for large-scale fading at 2.4 GHz.

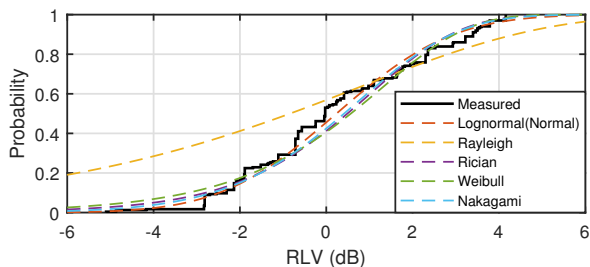


Fig. 6. CDF of relative loss variation for large-scale fading at 5.9 GHz.

log-normal, Rayleigh, Rician, Nakagami and Weibull distributions, as shown in Figs. 5 for 2.4 GHz and 6 for 5.9 GHz.

To show the Goodness of Fit (GoF) of those distribution functions to our measurements, we applied three different test metrics: Kolmogorov–Smirnov (KS), Chi-Square (Chi) and Maximum Likelihood Estimation (MLE), with results tabulated in Table III. The KS results suggest the log-normal distribution being the highest match percentage with big margins from the others. However, the Chi and MLE results show no dominance of the log-normal distribution and, in particular, the Chi results have demonstrate that Rician, Nakagami and Weibull are all better fitted than log-normal at 2.4 GHz. The parameters that represents the large-scale fading X_α as log-normal (normal in dB) for both frequencies are shared in Table IV.

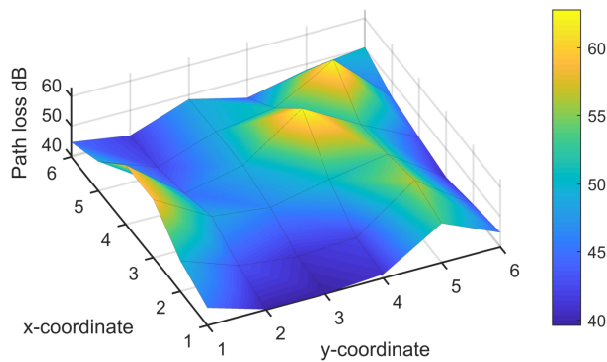


Fig. 7. A 3-dimensional view of the measured path loss in the grid at 2.4 GHz with 2 cm spacing.

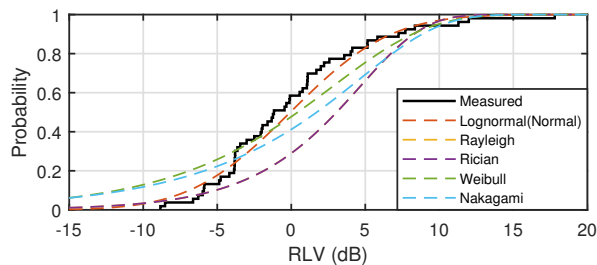


Fig. 8. CDF of relative loss variation for small-scale fading at 2.4 GHz.

C. Small-scale fading

Small-scale fading is defined as the variation of the received signal power over a short time period or a short distance less than a few wavelengths. The magnitude of this variation can be as high as 40 dB [10]. In our work, the intra-vehicle small-scale fading profile was investigated using two methods based on the measurements taken from a spatially tightened grid, as described below.

a) *Spatial distribution of path loss due to small-scale fading*: The received signal power was measured and later converted into the path loss for 36 locations as shown in Fig. 2. The distribution of the path loss for those location is shown by Fig. 7 in a three-dimensional view. The result shows a significant loss variation when the receiver is moved by just 2 cm. This behavior is due to the multipath characteristics of the channel and in particular due to the narrowband of signals transmitted. In addition, the largest variation in path loss measure at 55 dB, which is 15 dB above the mean loss of this grid, is observed.

b) *CDF for small-scale fading effect*: The small-scale fading component was extracted from the measured path loss from Test-1 as shown in Fig. 1, by deducting the large-scale fading component from the actual loss measurement which represents the relative loss variation (RLV) for small-scale fading. The small-scale fading effect was then demonstrated using the CDF of RLV in comparison with the same group of

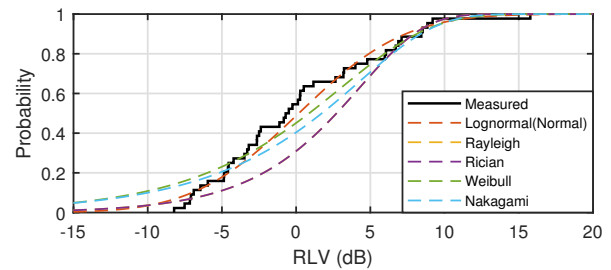


Fig. 9. CDF of relative loss variation for small-scale fading at 5.9 GHz.

TABLE V
PARAMETERS OF LOG-NORMAL DISTRIBUTION FOR SMALL-SCALE FADING (β_s) AT 2.4 GHz AND 5.9 GHz

Frequency(GHz)	Mean(dB)	Standard Deviation(dB)	Variance(dB)
2.4	-0.072	5.339	28.505
5.9	0.177	5.617	31.554

popular distribution functions, as shown in Fig. 8 for 2.4 GHz and Fig. 9 for 5.9 GHz.

By comparing the CDFs in Figs. 5 and 6 with those in Figs. 8 and 9, clearly small-scale fading lays a considerably dominant role over large-scale fading in contributing to the overall path loss in the intra-vehicle environment. The RLV caused by small-scale fading is significantly higher than that of large-scale fading and can reach as high as 18 dB.

To check the GoT among those distributions to the measured results, KS, Chi and MSE metrics were also used with the comparison results shown in Table VI. As indicated by KS and MLE results, the log-normal distribution is statistically a better fit than other types of distributions. Some statistical parameters for describing small-scale fading β_s as a log-normal distribution (normal in dB) for both frequencies are given in Table V.

The small-scale fading distributions for both frequencies appear to be similar to each other. This feature has been confirmed by using the two-sample KS test which demonstrates a

TABLE VI
GOODNESS OF FIT FOR SMALL-SCALE FADING (β_s)

Frequency: 2.4 GHz			
Distribution	KS	Chi	MLE
Log-normal	84.41%	24.68%	92.19%
Rayleigh	0.09%	15.4%	0.29%
Rician	0.09%	15.4%	0.29%
Weibull	14.41%	23.33%	5.81%
Nakagami	1.012%	21.19%	1.42%
Frequency: 5.9 GHz			
Distribution	KS	Chi	MLE
Log-normal	70.43%	23.14%	68.81%
Rayleigh	0.01%	15.73%	3.73%
Rician	0.01%	15.73%	3.73%
Weibull	24.58%	23.39%	15.50%
Nakagami	4.96%	22.02%	8.22%

TABLE VII
SMALL-SCALE FADING (β_s) TWO-SAMPLE-KS TEST

Frequency (GHz)	KS p-value	
	2.4(Estimated)	5.9(Estimated)
2.4(Estimated)	1	0.984
5.9(Estimated)	0.984	1

[10] A. Grami, "Chapter 12 - Wireless Communications," in Introduction to Digital Communications, 2015.

close correlation between the small-scale fading components β_s at 2.4 GHz and 5.9 GHz, as shown in Table VII. In other words, the path loss variation caused by small-scale fading is not significantly affected by the carrier frequency in this environment.

IV. CONCLUSION

The paper has presented the propagation characteristic of narrowband signals at 2.4 GHz and 5.9 GHz in the intra-vehicle wireless channels. Various channel parameters have been extracted from the received signal power measurements such as the distance-related attenuation loss or the mean loss, large-scale fading and small-scale fading statistics, which jointly contribute to the overall path loss. In addition, we have demonstrated that the small-scale fading effect is not statistically dependent on carrier frequency.

We have found that multipath fading has a significant impact on the path loss performance of narrowband signals compared to the attenuation-related loss which has a varied relationship with the free-space loss depending on the operating frequency chosen. We have also showed that small-scale fading is much more influential than large-scale fading on path loss in this environment. These findings will help to identify suitable technologies to mitigate the small-scale fading effect on data transmission in intra-vehicle wireless channels.

REFERENCES

- [1] F. Arena and G. Pau, "An Overview of Vehicular Communications," *Futur. Internet*, vol. 11, no. 2, p. 27, 2019.
- [2] J. Blumenstein et al., "In-vehicle channel measurement, characterization, and spatial consistency comparison of 3-11 GHz and 55-65 GHz frequency bands," *IEEE Trans. Veh. Technol.*, vol. 66, no. 5, pp. 3526–3537, 2017.
- [3] L. Cheng, J. Casazza, J. Grace, F. Bai, and D. D. Stancil, "Channel Propagation Measurement and Modeling for Vehicular In-Cabin Wi-Fi Networks," *IEEE Trans. Antennas Propag.*, vol. 64, no. 12, pp. 5424–5435, 2016.
- [4] R. Liu, S. Herbert, T. H. Loh, and I. J. Wassell, "A Study on Frequency Diversity for Intra-Vehicular Wireless Sensor Networks (WSNs)," in *Proc. IEEE Veh. Technol. Conf. (VTC Fall)*, 2011, pp. 1–5.
- [5] A. R. Moghimi, H. M. Tsai, C. U. Saraydar, and O. K. Tonguz, "Characterizing intra-car wireless channels," *IEEE Trans. Veh. Technol.*, vol. 58, no. 9, pp. 5299–5305, 2009.
- [6] H. Kamoda, S. Kitazawa, N. Kukutsu, K. Kobayashi, and T. Kumagai, "Microwave propagation channel modeling in a vehicle engine compartment," *IEEE Trans. Veh. Technol.*, vol. 65, no. 9, pp. 6831–6841, 2016.
- [7] T. S. Rappaport, *Wireless Communications Principles and Practice*, 2nd ed., Prentice Hall: Upper Saddle River, NJ, USA, 2002.
- [8] A. C. Rencher and G. B. Schaalje, *Linear Models in Statistics*, 2nd ed., Wiley, 2008.
- [9] D. de la Vega et al., "Generalization of the Lee method for the analysis of the signal variability," *IEEE Trans. Veh. Technol.*, vol. 58, no. 2, pp. 506–516, 2009.